$CO_2^{\bullet -}$ Radical Induced Cleavage of Disulfide Bonds in Proteins. A γ-Ray and Pulse Radiolysis Mechanistic Investigation†

Vincent Favaudon,*,‡ Hervé Tourbez,‡ Chantal Houée-Levin,§ and Jean-Marc Lhoste‡

Unité 219 INSERM, Institut Curie-Biologie, Centre Universitaire, 91405 Orsay Cedex, France, and Laboratoire de Chimie-Physique, Université René-Descartes, 45 Rue des Saints-Pères, 75270 Paris Cedex 06, France

Received March 21, 1990; Revised Manuscript Received August 1, 1990

ABSTRACT: Disulfide bond reduction by the $CO_2^{\bullet -}$ radical was investigated in aponeocarzinostatin, apo-riboflavin-binding protein, and bovine immunoglobulin. Protein-bound cysteine free thiols were formed under γ-ray irradiation in the course of a pH-dependent and protein concentration dependent chain reaction. The chain efficiency increased upon acidification of the medium, with an apparent pK_a around 5, and decreased abruptly below pH 3.6. It decreased also at neutral pH as cysteine accumulated. From pulse radiolysis analysis, $CO_2^{\bullet -}$ proved able to induce rapid one-electron oxidation of thiols and of tyrosine phenolic groups in addition to one-electron donation to exposed disulfide bonds. The bulk rate constant of $CO_2^{\bullet -}$ uptake by the native proteins was 5- to 10-fold faster at pH 3 than at pH 8, and the protonated form of the disulfide radical anion, (S$\underline{\overset{\bullet}{-}}$S)H, appeared to be the major protein radical species formed under acidic conditions. The main decay path of (S$\underline{\overset{\bullet}{-}}$S)H consisted of the rapid formation of a thiyl radical intermediate S$^{\bullet}$ HS in equilibrium with the closed, cyclic form. The thiyl radical was subsequently reduced to the sulfhydryl level SH HS on reaction with formate, generating 1 mol of the $CO_2^{\bullet -}$ radical, thus propagating the chain reaction. The disulfide radical anion S$\underline{\overset{\bullet -}{-}}$S at pH 8 decayed through competing intramolecular and/or intermolecular routes including disproportionation, protein–protein cross-linking, electron transfer with tyrosine residues, and reaction with sulfhydryl groups in prereduced systems. Disproportionation and cross-linking were observed with the riboflavin-binding protein solely. Formation of the disulfide radical cation S$\underline{\overset{\bullet +}{-}}$S, phenoxyl radical Tyr–O$^{\bullet}$ disproportionation, and phenoxyl radical induced oxidation of preformed thiol groups should also be taken into consideration to explain the fate of the oxygen-centered phenoxyl radical.

Due primarily to the versatility of its electronic properties, sulfur plays a major role in the chemistry of life. It may, for instance, serve as a terminal electron acceptor, as in sulfate-reducing bacteria, participate in a variety of key metabolic processes, like those involving ubiquitous glutathione, or, in the form of methionine and cysteine, be incorporated within the amino acid backbone of proteins. Cysteine free sulfhydryl groups may be part of catalytic sites, as in cytochrome P-450, iron–sulfur centers, or certain proteolytic enzymes. Cysteine is also prone to establish disulfide bridges by oxidation, thereby resulting in cross-linking of individual peptide chains, as in insulin, α-chymotrypsin, or immunoglobulins, or contributing to the stabilization of globular proteins conformation by intrachain covalent binding. The cystine disulfide bond is not chemically inert and may have a catalytic role, as in thioredoxin and in the flavoenzyme glutathione reductase. Unfortunately, no conventional chemical method has proven to be of general purpose for the investigation of the structure and function of disulfide bonds in proteins. Though of common use, thiol–disulfide exchange, e.g., with 2-mercaptoethanol, depends on many factors such as steric hindrance, relative redox potentials and concentrations, pH, or temperature, some of which are not taken into account or poorly controlled most of the time. Furthermore, this method hardly affords kinetic informations.

Radiolytic techniques may offer an alternative for probing disulfide bond reactivity in proteins. That is the case in particular for the carboxyl radical $CO_2^{\bullet -}$. This species is obtained in pure form, with a radiolytic yield of 0.62 μmol·J^{-1}, by scavenging with formate ion and nitrous oxide the radicals formed in the course of water radiolysis:

$$e_{aq}^- + N_2O\ (+ H_2O) \rightarrow OH^{\bullet} + OH^- + N_2$$

$$OH^{\bullet} + HCOO^- \rightarrow CO_2^{\bullet -} + H_2O$$

$$H^{\bullet} + HCOO^- \rightarrow CO_2^{\bullet -} + H_2$$

The carboxyl radical is known as a powerful one-electron donor whose standard redox potential in the $CO_2/CO_2^{\bullet -}$ couple is −1.85 V (Surdhar et al., 1989). Electron donation from $CO_2^{\bullet -}$ to proteins devoid of electron-affinic cofactors, such as hemes or flavins, has long been proposed to be selectively confined to the disulfide bonds (Adams et al., 1972). Disulfide groups are also able to trap by internal electron transfer excess free electrons resulting from e_{aq}^- attack at other groups in proteins, thus acting as electron sinks (Rao et al., 1983). Actually, the carboxyl radical reacts with low molecular weight linear or cyclic disulfide (dithiane) compounds RSSR (Adams, 1967; Willson, 1970; Elliot et al., 1984; Wu et al., 1984) and with cystine groups in proteins as well (Adams et al., 1972; Faraggi & Klapper, 1988) with rate constants of the order of 10^8 M^{-1}·s^{-1}. The primary product of this electron-transfer

† We are indebted to the Ministère de la Recherche et de la Technologie for funding the linear electron accelerator installation. This work was supported by financial aid from the Institut National de la Santé et de la Recherche Médicale and by a grant (89-21-5) from the Institut Curie.

‡ Institut Curie-Biologie.

§ Université René-Descartes.

0006-2960/90/0429-10978$02.50/0

reaction at neutral pH is the disulfide (dithiane) radical anion $RSSR^{\bullet-}$ characterized by an intense absorption around 400 nm. The protonated form of this radical, $(RSSR)H^{\bullet}$, which occurs with an apparent pK_a estimated at 5.2–5.5 (Chan & Bielski, 1973; Redpath, 1973; Elliot & Sopchyshyn, 1982) shows a weaker absorption peaking also at 400 nm (Akhlaq & von Sonntag, 1987). However, the carboxyl radical may also act as a strong oxidant, with a standard redox potential relative to the $CO_2^{\bullet-}/HCOO^-$ couple estimated at +1.1 to +1.5 V (Koppenol & Rush, 1987; Surdhar et al., 1989).

We report here a γ-ray and pulse radiolysis study of $CO_2^{\bullet-}$-induced free-radical formation and decay in three proteins of markedly different structure and disulfide bond content, namely, (i) aponeocarzinostatin (NCS), a small (M_r = 10700) single-chain antitumor antibiotic carrier containing two disulfide bonds and no histidine residue according to amino acid sequence determinations (Maeda et al., 1974; Gibson et al., 1984), (ii) apo-riboflavin-binding protein (RBP) from hen egg white (M_r = 29200), a single-chain glycoprotein containing nine disulfide bonds (Kumosinski et al., 1982; Hamazume et al., 1984) located at or near the protein surface (Kozik, 1982), and (iii) bovine immunoglobulin (IgG), a large (M_r = 164000) complex formed from two heavy and two light chains held together by disulfide bridges. None of these (apo)proteins contains free cysteine in the native form. We show that the $CO_2^{\bullet-}$ radical in these systems develops a dual character. It works as a reductant by electron attachment to disulfide groups; it also induces oxidization of tyrosine residues, thereby generating the phenoxyl radical Tyr–O$^{\bullet}$. The disulfide radical anion, though itself a strong reductant with a redox potential of ca. −1.3 V for the S–S/S$^{\bullet-}$–S couple (Surdhar & Armstrong, 1986, 1987), appears to be relatively long-lived in proteins. The decay of S$^{\bullet-}$–S and of the protonated form (S$^{\bullet-}$–S)H involves at least five different pathways including S–S bond opening with formation of the thiyl radical S$^{\bullet}$ HS, disproportionation, reaction with Tyr–O$^{\bullet}$ radicals, cross-linking, and free thiol induced deactivation. The relative probabilities of these processes depend on the nature of the protein as well as on the pH, on the protein concentration, on the presence of free thiols, and, in pulse radiolysis experiments, on the radiation dose per pulse. Acidic catalysis, suggesting the formation of a labile intermediate complex held by heteropolar interactions, also appears in the formation of (S$^{\bullet-}$–S)H.

Experimental Procedures

(*1*) *Products.* Formic acid, sodium formate, and dipotassium hydrogen phosphate were of the highest quality available and were used as received. [^{35}S]Cysteine (specific activity 3.20 GBq·mmol^{-1}) was obtained from Amersham. Water was purified through a Spectrum system and subsequently distilled in a quartz apparatus.

(*2*) *Proteins.* Aponeocarzinostatin (NCS)[1] was extracted from the culture broth of *Streptomyces carzinostaticus var. F41* (ATCC 15944) as described (Favaudon, 1983). Apo-riboflavin-binding protein (RBP) was purified from White Leghorn hen eggs following minor modifications to the procedure of Blankenhorn et al. (1975), including affinity chromatography on EAH-Sepharose 4B substituted with riboflavin 3-acetate by a carbodiimide coupling method. Riboflavin 3-acetate was a generous gift of Dr. Sandro Ghisla, University of Konstanz, West Germany. NCS and RBP were found to be free of contaminants through SDS–PAGE and isoelectric focusing analysis. Bovine IgG (mostly IgG_1) was obtained in >95% pure form from commercial γ-globulin preparations (Cohn fraction II/III, Sigma) by gel filtration over Sephacryl S-300 (Pharmacia) or Ultrogel AcA-34 (IBF). The protein concentrations were measured spectrophotometrically by using the following molar extinction coefficients: NCS, ϵ_{273} = 13.8 mM^{-1}·cm^{-1} (Povirk et al., 1981); RBP, ϵ_{278} = 50.0 mM^{-1}·cm^{-1} (Blankenhorn et al., 1975); bovine IgG, ϵ_{278} = 185 mM^{-1}·cm^{-1}, determined from Bradford protein titration (Bradford, 1976) using an IgG standard as reference. Stock solutions of proteins were dialyzed extensively against 100 mM sodium formate and stored at −20 °C.

(*3*) *Sulfhydryl Group Processing.* Free sulfhydryl groups were determined by optical titrations with DTNB at pH 7.9 (100 mM Tris-HCl buffer), using ϵ_{410} = 13.6 mM^{-1}·cm^{-1} for the 3-carboxylato-4-nitrothiophenolate anion (Ellman, 1958). Alkylation of thiol groups in proteins was usually achieved by reaction with 10 mM iodoacetamide; the reaction was over within a 5-min incubation at room temperature.

(*4*) *Electrophoresis.* Isoelectric focusing was done by using a flat bed (PhastSystem, Pharmacia) electrophoresis unit. SDS–PAGE in discontinuous buffer system, with or without a gradient of polyacrylamide concentration, was performed in the absence of 2-mercaptoethanol by using the PhastSystem or a vertical (LKB Model 2001) electrophoresis unit. Cysteine free thiol groups released upon irradiation were alkylated with iodoacetamide prior to running the electrophoreses. Both Coomassie blue and silver staining methods were used, depending on the conditions, and high-resolution scanning of stained gels was subsequently made on an UltroScan XL laser densitometer (LKB). Thiol alkylation was also done by using a 2-fold molar excess of the fluorogenic label *N*-[7-(dimethylamino)-4-methyl-3-coumarinyl]maleimide (Serva) as described (Goto & Aki, 1984); labeled proteins were then revealed as fluorescent bands under ultraviolet illumination.

(*5*) *γ-Ray Irradiations.* γ-Ray irradiations were carried out at 25–27 °C with a cobalt-60 source, at dose rates comprised between 22.0 and 25.3 Gy·min^{-1}. Radiation doses were calibrated by Fricke's procedure. Samples to be irradiated were contained in 10-mL Erlenmeyer flasks fitted with septum inlet adapters. N_2O (99.99%; <20 ppm O_2) was saturated with water and introduced through the septums by using stainless steel tubings penetrating down to a few millimeters over the liquid surface, avoiding bubbling and contact with the solutions. Gas equilibration ($[N_2O] \approx 25$ mM, 25 °C) was allowed to proceed by flushing for at least 60 min in dim light under permanent stirring or vortexing. The amount of residual oxygen in the solution was estimated at less than 25 nM by using methyl viologen as described earlier (Favaudon et al., 1985). For studies as a function of the dose of γ-rays, aliquots were taken anaerobically at time intervals using a gas-tight syringe, chilled, and processed within a few minutes. Unless otherwise stated, samples to be irradiated were made up in 20 mM dipotassium hydrogen phosphate–100 mM sodium formate buffer adjusted to the pH required with formic acid.

(*6*) *Radiation-Induced Cross-Linking of [^{35}S]Cysteine to RBP.* Mixtures of 50 μM RBP and 250 μM [^{35}S]cysteine were made up in phosphate–formate buffer at pH 8.13 or 5.82 and irradiated stepwise under N_2O, up to 150 Gy of γ-rays.

[1] Abbreviations: NCS, aponeocarzinostatin; RBP, apo-riboflavin-binding protein; IgG, bovine immunoglobulins G; Tris, tris(hydroxymethyl)aminomethane; DTNB, 5,5′-dithiobis(2-nitrobenzoate); SDS–PAGE, polyacrylamide gel electrophoresis with lauryl sulfate; Cys–SH, protein-bound cysteine groups; S–S, protein-bound, cyclic disulfide groups and derivatives thereof.

Aliquots were taken anaerobically, treated immediately with iodoacetamide in excess, and submitted to gel filtration over Sephadex G-25 microcolumns. The pooled protein fractions were titrated spectrophotometrically, and the radioactivity was counted by scintillation.

(*7*) *Preparation of Half-Reduced–Alkylated RBP.* RBP (100 μM) in phosphate–formate buffer, pH 6.0, was sequentially reduced by γ-ray irradiation (20 Gy·min^{-1}) up to 50% with respect to the total disulfide content, incubated with saturating iodoacetamide, filtered through Sephadex G-25 to remove excess reactant, dialyzed against phosphate–formate buffer, pH 8.20, concentrated by centrifugation over Centricon-10 microconcentrators (Amicon), and finally adjusted to the desired protein concentration.

(*8*) *Pulse Radiolysis Experiments.* Pulse radiolysis was performed with newly set-up equipment at the Institut Curie-Biologie, Orsay. The system is based on the Kinetron, a remarkably compact 4.5-MeV linear electron accelerator designed by the CGR-MeV company, now a subsidiary of General Electric Inc. The accelerating guide of the Kinetron is powered by a magnetron (3-GHz band, 2.5 MW peak power). The electron gun (11 kV accelerating potential) is of the triode type, permitting instant adjustment of the beam current (10–250 mA) and pulse width (0.05–2.7 μs) with ease and reliability. A single electron pulse most currently involves a total of three successive microwave pulses at a 16.66 ± 0.01 ms interval with electron injection during the last microwave pulse. The pulse-to-pulse reproducibility thus obtained is better than ±5%. There is a no preirradiation of the sample and no need for an electromagnetic deflection of the output electrons. The apparatus is operated by a microcomputer via an optoelectronic interface designed and built by one of us (H.T.), permitting an automated control of the pulse sequences, delays, triggering, and dosimetry. The maximum dose per pulse is in the range of 60 Gy.

A poly(methyl methacrylate) optical fiber is disposed on the edge of the electron beam. The flash of Cerenkov light formed in this fiber at the time of the 4.5-MeV electron pulse permits real-time detection of the pulse profile using a photomultiplier with a 50-Ω load. Furthermore, the area of the Cerenkov peak appears to be proportional to the number of electrons received in the irradiation cell. This method, which keeps the shot noise to a negligible level, can thus be used as a routine dosimeter. Calibration was made by comparison with the transient absorption of an air-saturated KSCN dosimeter [10 mM KSCN, $G(SCN)_2^{\bullet -}$ = 0.30 μmol·J^{-1}, ϵ_{472} = 7.4 mM^{-1}·cm^{-1}]. The homogeneity of the irradiation field, determined by using lithium fluoride thermoluminescent dosimeters and wide contrast photographic films, is better than ±3%.

The optical assembly for the determination of transmittance changes following pulse irradiation comprises the following: (1) two light sources, a stabilized 150-W tungsten–halogen bulb on one hand and a (pulsed) 150-W xenon arc on the other, with achromatic doublet or fused silica (Suprasil grade) condensing lenses, respectively, (2) a remotely actuated right-angle crown glass prism used as total internal reflector for light source commutation, (3) low-pass filters and a remotely activated shutter, (4) the irradiation cell, (5) a Suprasil collecting lens, (6) two antiparallel plane UV grade mirrors, and (7) a Jobin-Yvon H-25 monochromator fitted with a homofocal Suprasil focusing lens, a holographically recorded plane reflection grating, and a Hamamatsu R-928 photomultiplier. The distance covered by the light beam is ca. 5 m, including passage through the 1.2 m thick concrete shield. The irradiation cell is disposed in such a way that the electron and light beams lie at 90° from each other in the horizontal plane. The cell is made of fused silica (Suprasil) and has 1.25 mm thick optically flat windows. The path lengths are 2 and 10 mm along the electron and light beams, respectively. The aperture along the light beam is of 2 × 5 mm. Each run requires 125 μL of fresh solution.

Samples for pulse radiolysis experiments were prepared and saturated with N_2O in the same way as described above for γ-ray irradiation and transferred anaerobically to an N_2O-flushed irradiation cell closed by a rubber septum, using a modified Hamilton syringe. Absorbed doses were in the range of 2–52 Gy per pulse.

The output data from the photomultiplier circuitries are stored in a Nicolet 4094C digital oscilloscope comprising a 4180/2 (200 MHz sampling rate, 8 bits resolution) and a 4570 (10 MHz sampling rate, 12 bits resolution) plug-in unit operated in parallel, using a 2^{12} data points format. The data are subsequently transferred to a Nicolet XF-44/2 floppy disk memory and to an Apple MacIntosh II computer via an IEEE-488 parallel interface. For kinetic analysis, samples of 100–1000 data points (absorbance values) were taken and fitted to different systems of rate equations. No smoothing was applied. Linear least-squares regression analysis was used for pure first- (exponential) or second-order (hyperbolic) time dependencies. Solving nonlinear time-dependent functions in accordance with the least-squares criterion was done by using iterative approximation techniques. Iterative computer routines based on the Gauss–Levenberg–Marquardt algorithm are of interest for fitting integrated rate equations to experimental data for they are simple to program, save computer time, tolerate crude starting values of the parameters, and have been described extensively in textbooks (Press et al., 1988). Finding solutions to multiexponential systems with this approach is no problem. The deconvolution of mixed (pseudo-) first-order and second-order reactions by this method was carried out according to Gorman and Connolly (1973).

Results and Discussion

(*1*) *γ-Ray Radiolysis.* In this first section we present the results obtained under steady-state conditions from conventional γ-ray irradiation experiments, as a function of pH, radiation dose, and protein concentration. We also analyze disulfide bond cleavage in IgG by electrophoresis and give evidence of radiation-induced cross-linking in partly reduced RBP.

(*1.1*) *pH and Protein Dependence of Disulfide Bond Cleavage.* Protein-bound DTNB-titrable cysteine thiol groups (Cys–SH) were formed upon γ-ray irradiation of NCS, RBP, and bovine IgG in N_2O-saturated formate. Figure 1A shows a typical pattern of reduction obtained with RBP. At low pHs, the reaction proceeded rapidly up to complete reduction of the nine disulfide bonds present in native RBP, with concomitant loss of the riboflavin-binding capacity. At higher pHs, part only (ca. 40%) of the disulfide bonds of the protein was cleaved upon prolonged (>1 kGy) irradiation. Resuming irradiation under N_2O after acidification of such preirradiated, partly reduced neutral solutions of RBP resulted in the rapid, stoichiometric release of Cys–SH (Figure 1B). No detectable dihydrogen sulfide was released at any pH. In fact, the loss of disulfide bonds and the half-formation of Cys–SH were always equal within experimental error. Figure 1A shows also that the rate of Cys–SH formation decreased as the radiation dose was raised. This inhibitory effect was mostly pronounced at pH 8.0–8.2. Bovine IgG showed a pattern very similar to that observed with RBP, with a total of 7 mol of reducible disulfide groups per mole of protein.

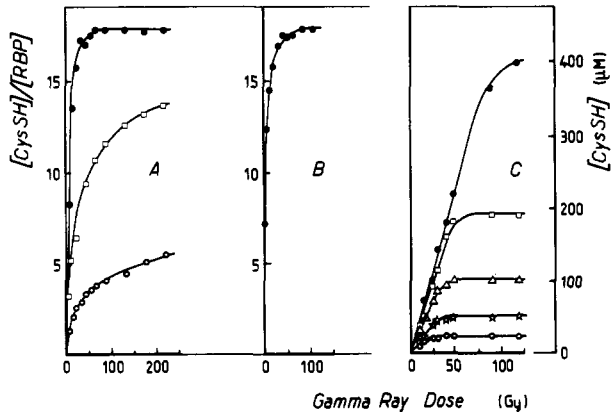

FIGURE 1: γ-Ray dose dependence of the formation of DTNB-titrable cysteine sulfhydryl groups in RBP (A, B) and NCS (C). (A) Reduction of 10 μM RBP at pH 3.80 (●), pH 5.98 (□), or pH 8.09 (○). (B) Reduction of 10 μM RBP at pH 3.82 following a 450-Gy preirradiation at pH 8.09. (C) Reduction of 12.5 μM (○), 25 μM (☆), 50 μM (△), 100 μM (□), and 200 μM (●) NCS at pH 7.40. Experiments were performed in N_2O-saturated 20 mM phosphate–100 mM formate buffer at a γ-ray dose rate of 25.3 Gy·min^{-1}.

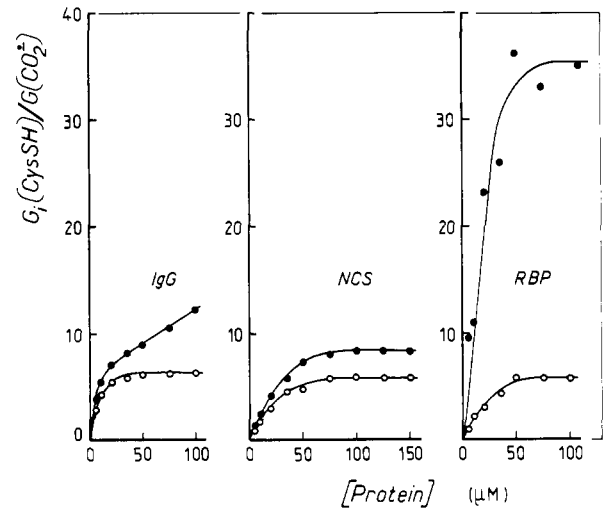

FIGURE 2: Effect of the protein concentration on the initial yield of sulfhydryl group formation at pH 7.78 (○) and pH 4.00 (●). The conditions for γ-ray irradiation were as in Figure 1. The initial yield of Cys–SH is given relative to the radiolytic yield (0.62 μmol·J^{-1}) of the carboxyl radical.

The behavior of NCS is markedly different from that of the other two proteins since the reaction always proceeded to completion at neutral pH (Figure 1C). Two moles only of Cys–SH were released per mole of NCS at the plateau of the reaction. One out of the two disulfide bonds of NCS appears, therefore, to be resistant to $CO_2^{\bullet -}$-induced cleavage.

Figure 2 summarizes the effect of the protein concentration on the initial yield of Cys–SH formation at two representative pHs ([$HCOO^-$] = 100 mM). It appears from the value of the initial yield of Cys–SH formation, G_i(Cys–SH), that $CO_2^{\bullet -}$-induced cleavage of disulfide bonds in the three proteins of interest is a chain reaction, as reported earlier for the oxidized (cyclic) forms of dithiothreitol and lipoamide (Elliot & Sopchyshyn, 1982; Wu et al., 1984). This chain reaction is highly dependent on the pH and on the nature of the protein and, with the exception of IgG at acid pH, shows unusual plateau values at high protein concentration. The more efficient chain is that formed with RBP at pH 4.0, where 35 mol of Cys–SH groups are produced per mole of $CO_2^{\bullet -}$ radical at saturating protein concentration. At pH 7.8 the three proteins show a similar profile of the G_i(Cys–SH) vs protein concentration curve, with a plateau corresponding to the release of 6.0 ± 0.4 mol of Cys–SH per mole of $CO_2^{\bullet -}$ radical. At this pH, G_i(Cys–SH) at high protein concentration does not change significantly upon varying the γ-ray dose rate between 17 and 42 Gy·min^{-1} but increases linearly [G_i(Cys–SH)/[$HCOO^-$] = 32 μL·J^{-1}, RBP] with the formate ion concentration ([$HCOO^-$] ≥ 50 mM).

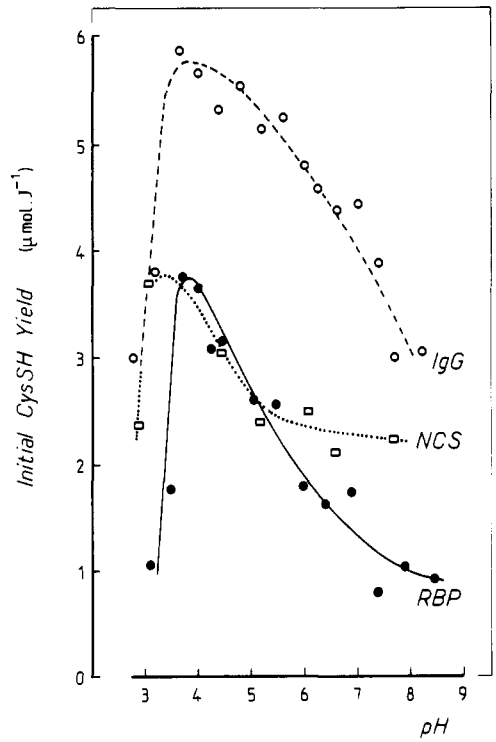

FIGURE 3: pH dependence of the initial yield of Cys–SH formation in 30 μM IgG (○- - -), 25 μM NCS (□···), and 10 μM RBP (●—) samples. γ-Ray irradiation was performed as explained in the legend to Figure 1.

A plot of G_i(Cys–SH) vs pH is shown in Figure 3. The result is reminiscent of that reported by Elliot et al. (1984) in the case of dithiothreitol and glutathione. It suggests the existence of an intermediate with a pK_a in the range of pH 5–6, most likely corresponding to the disulfide radical (Chan & Bielski, 1973; Redpath, 1973; Elliot & Sopchyshyn, 1982; Akhlaq & von Sonntag, 1987). The sudden fall in G_i(Cys–SH) below pH 3.5 (Figure 3) is attributed to protonation of the formate ion $HCOO^-$ and attendant inhibition of chain propagation (Elliot et al., 1984).

(1.2) Electrophoretic Analysis of Bovine IgG Fragments. Aliquots of a solution of bovine IgG irradiated with γ-rays for various times in N_2O-saturated phosphate–formate buffer, pH 6.0, were taken anaerobically and treated by thiol-specific reagents in one of three ways, namely, (i) by DTNB for titration of released Cys–SH, showing a nonlinearly dose-related curve as in Figure 1A, (ii) by a 2-fold molar excess, relative to Cys–SH, of the fluorogenic reagent *N*-[7-(dimethylamino)-4-methyl-3-coumarinyl]maleimide for 20 min at room temperature, or (iii) by addition of a 1/10 volume of 100 mM iodoacetamide (10-min incubation, room temperature). Protein–coumarinyl conjugates were first isolated by gel filtration over Sephadex G-25. They showed an absorption band at 395 nm, with a molar extinction coefficient (ϵ_{395} = 19.8 mM^{-1}·cm^{-1}) close to that of the free chromophore and an intense fluorescence emission at 470 nm. SDS–PAGE analysis of coumarinyl-substituted IgG displayed sharp fluorescent bands under ultraviolet illumination with apparent molecular weights corresponding to those of isolated light (L, M_r =

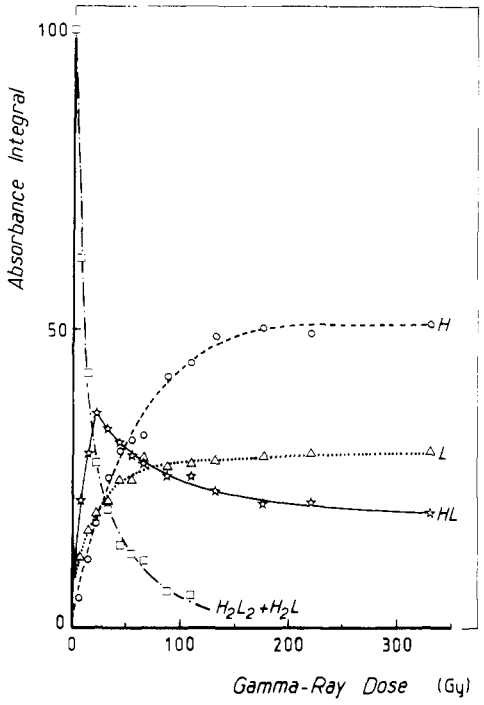

FIGURE 4: SDS–PAGE analysis of the $CO_2^{\bullet-}$-induced cleavage of interchain disulfide bridges in bovine IgG. Electrophoresis, Coomassie blue staining, and densitometric measurements were carried out as described under Experimental Procedures. The integral optical density in each lane was taken at 100%. IgG was 25 μM (pH 6.1).

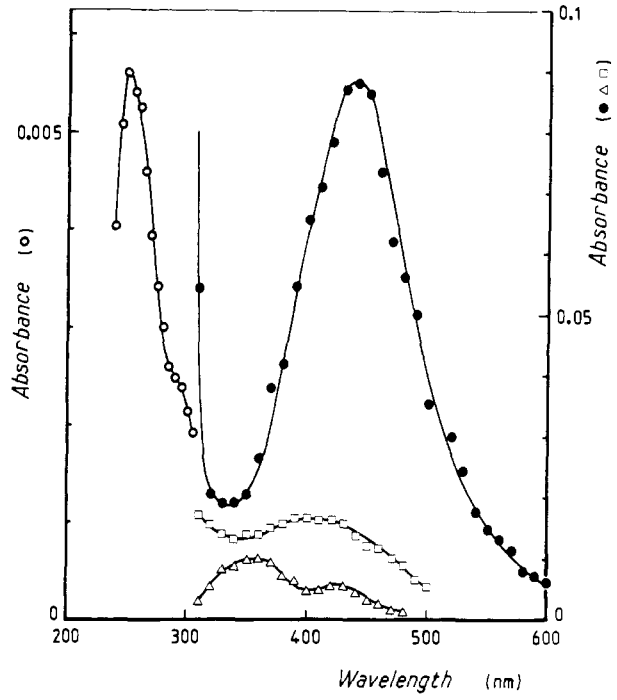

FIGURE 5: Transient absorption spectra formed upon pulse radiolysis of IgG solutions in N_2O-saturated phosphate–formate buffer. (●) 200 μM IgG, pH 8.09, 42.0 ± 1.7 Gy, time after the pulse 250 μs; (○) 4 μM IgG, pH 8.23, 36.9 ± 1.5 Gy, time after the pulse 400 μs; (□) 250 μM IgG, pH 3.36, 36.9 ± 1.5 Gy, time after the pulse 12 μs; (△) 250 μM IgG, pH 3.34, 36.9 ± 1.5 Gy, time after the pulse 2 ms. The optical path length was of 10 mm. The maximum absorption wavelengths and molar extinction coefficients of the compounds formed are given in Table I.

25 200) and heavy (H, M_r = 57 000) chains and to HL (M_r = 82 000) and H_2L (M_r = 115 000) fragments. The uncleaved IgG molecule, H_2L_2 (M_r = 164 000), was not labeled. This indicates that $CO_2^{\bullet-}$-induced scission of the interchain disulfide bridges precedes cleavage of intradomain disulfide bonds. Attack of intradomain bonds seemed to occur only in isolated H and L fragments at high radiation doses.

Irradiated samples (pH 6.1) of bovine IgG were also alkylated with iodoacetamide and submitted to SDS–PAGE. The densitometric analysis of slab gels stained with Coomassie blue R-250 showed, concomitantly with the disappearance of H_2L_2 and H_2L forms, the formation of the half-IgG molecule HL and of isolated light (L) and heavy (H) chains (Figure 4). The release of the HL complex was initially faster than that of the H or L fragments, and part only of the HL form decayed at higher doses, up to a steady-state representing about 19% of the initial IgG concentration on a molar basis.

(1.3) RBP Cross-Linking. $CO_2^{\bullet-}$-induced formation of interprotein disulfide linkages has been described a few years ago for bovine serum albumin by Schuessler and Freundl (1983). Due to steric factors, such recombination processes may be favored within the IgG complex, thus explaining the persistence of a large amount of the HL form at high radiation doses (Figure 4). No dimerization occurred with NCS, even after exposure to doses in the 10-kGy range. The cross-linking reaction was thus investigated by taking RBP as a model. This was done using two methods. First, SDS–PAGE analysis of a 300 μM solution of RBP which had been given high doses of γ-rays under N_2O in phosphate–formate buffer, pH 8.21, showed the appearance of a new band with exactly the molecular mass (M_r = 64 000) expected of a dimer of RBP. This species amounted to 16% of the total protein concentration (based on Coomassie R-250 staining) for a dose of 1.3 kGy. It disappeared upon postirradiation treatment with 2-mercaptoethanol. Second, irradiation of mixtures of native RBP (50 μM) and free [^{35}S]cysteine (250 μM) resulted in the incorporation of [^{35}S]cysteine into RBP (see Experimental Procedures). The yield of cross-linking was found to increase linearly with the radiation dose for up to 100 Gy. The reaction was nearly twice as fast at pH 5.82 (0.35 mmol of [^{35}S]cysteine·Gy^{-1}·mol of RBP^{-1}) as at pH 8.13 (0.18 mmol of [^{35}S]cysteine·Gy^{-1}·mol of RBP^{-1}) representing, respectively, 2.7% and 1.4% of the integral amount of $CO_2^{\bullet-}$ formed upon irradiation.

(2) Pulse Radiolysis Studies. The experiments reported in this second section aim at the identification of the nature of radical intermediates and at the elucidation of their mechanisms of formation and decay. For the sake of clarity, formation and breakdown of radicals in the proteins under various conditions are described separately.

(2.1) Spectral and Kinetic Analysis of Radical Formation. (2.1.1) Radical Formation at pH 8.10–8.25. Pulsed attack of the native proteins by $CO_2^{\bullet-}$ at pH 8.10–8.25 gave rise to a biphasic reaction, with the rapid formation (phase I) of a transient optical absorption culminating in 200–400 μs and decaying subsequently (phase II) at a 500- to 2000-fold lower rate. For example, the absorption spectrum taken at the buildup of phase I from IgG (Figure 5) showed a sharp peak at 250 nm, a shoulder at 290 nm, a minimum at 335 nm, and an intense absorption band at 440 nm (425 nm in the case of NCS and RBP). The 425–440-nm band can be assigned to the disulfide radical anion $\underline{S^{\bullet-}S}$ formed from $CO_2^{\bullet-}$-induced reduction of cystine groups $\underline{S-S}$ in the same way as in low molecular weight linear or cyclic disulfides (Karmann et al., 1969; Caspari & Granzow, 1970; Hoffman & Hayon, 1972; Chan & Bielski, 1973; Wu et al., 1984; Akhlaq & von Sonntag, 1987; Akhlaq et al., 1989; Prütz et al., 1989). The absorption spectra of cyclic disulfide radical anions are subject to large variations in both the position of the maximum ab-

Table I: Equilibrium and Rate Constants Characteristic of the $CO_2^{\bullet -}$-Induced Formation of Radicals in NCS, IgG, and RBP[a]

	NCS	IgG	RBP
n	1	7	9
$k_2 + k_3$ ($M^{-1}\cdot s^{-1}$)	$(0.42 \pm 0.08) \times 10^8$	$(1.36 \pm 0.18) \times 10^8$	$(1.73 \pm 0.22) \times 10^8$
k_I ($M^{-1}\cdot s^{-1}$)	2.25×10^8	13.0×10^8	11.6×10^8
ϵ_{pH8} ($M^{-1}\cdot cm^{-1}$) [λ_{max} (nm)]	1450 ± 230 [425]	3340 ± 260 [440]	3890 ± 420 [425]
ϵ_{pH3} ($M^{-1}\cdot cm^{-1}$) [λ_{max} (nm)]	490 ± 35 [400]	780 ± 70 [400]	1090 ± 70 [400]
A_{250}/A_{410}	4.4 ± 0.7	3.7 ± 0.7	2.6 ± 0.4
$pK_{E.1}$	5.72	6.46	4.75
$pK_{E.2}$		5.49	
$pK_{E.3}$		4.45	
$pK_{R.1}$	4.51	5.33	4.51
$pK_{R.2}$		3.80	
$pK_{R.3}$		3.78	

[a] n is the number of $CO_2^{\bullet -}$-reducible disulfide bonds per mole of protein. $k_2 + k_3$, ϵ_{pH8} and k_I, ϵ_{pH3} are the total rate constants and mean molar extinction coefficients determined in basic (pH 8.10–8.25) and acidic (pH 3.03–3.36) media, respectively. k_I corresponds to reactions 2, 3, 5, and 6 in parallel. $k_2 + k_3$ and ϵ_{pH8} were calculated from data obtained under pseudo-first-order conditions from an average over 17 (NCS), 18 (IgG), and 16 (RBP) experiments while monitoring the protein concentration. ϵ_{pH3} was determined from the values of absorbance taken at the buildup of phase I ($t \approx 15$ μs) after deconvolution from phase II in a biexponential fit. k_I and the pK_a values relative to the pH dependence of the molar absorptivity at the plateau of phase I (pK_E) or to the apparent rate constant of $CO_2^{\bullet -}$ uptake in phase I (pK_R) were calculated for best fit with the experimental data (Figure 7). The A_{250}/A_{410} ratio was appreciated from experiments (pH 8.10–8.25) performed at low protein concentration. Second-order rate constants are given relative to the total protein concentration.

sorption wavelengths and the value of the molar extinction coefficients ($\epsilon_{410-425}$ = 4–9 $mM^{-1}\cdot cm^{-1}$) (von Sonntag, 1990). This makes it difficult to appreciate the $\underline{S^{\bullet -}S}$ content in the presence of other absorbing radical intermediates. However, $\underline{S^{\bullet -}S}$ has no large absorption at 250 nm and no shoulder at 290 nm. The 250–290-nm doublet may then be assigned (Feitelson & Hayon, 1973; Bent & Hayon, 1975) to the phenoxyl radical Tyr–O• resulting from oxidization of tyrosine residues. The Tyr–O• radical is also known to present, in addition to the 250–290-nm doublet, a well-defined absorption at 395–410 nm with an extinction coefficient in the range of 3 $mM^{-1}\cdot cm^{-1}$ (Feitelson & Hayon, 1973; Bent & Hayon, 1975; Bansal & Fessenden, 1976). We may therefore reasonably agree that Tyr–O• and $\underline{S^{\bullet -}S}$ both concur to the 425–440-nm absorption band, the contribution of the Tyr–O• radical at these wavelengths probably being minor compared to that of the $\underline{S^{\bullet -}S}$ radical. We tried to assess the relative amount of Tyr–O• and $\underline{S^{\bullet -}S}$ from the A_{250}/A_{410} ratio of absorbance at the plateau of phase I (200–400 μs). Despite the lack of precision inherent in the use of low protein concentrations in these experiments, there appears to be a striking correlation between the value of A_{250}/A_{410}, the bulk extinction coefficient (ϵ_{pH8}) of the mixed radical intermediates, and the bimolecular rate constant ($k_2 + k_3$) for the formation of these radicals in the proteins (Table I). These data suggest that the [Tyr–O•]/[$\underline{S^{\bullet -}S}$] ratio is determined by individual rate constants of tyrosine and disulfide groups for $CO_2^{\bullet -}$ uptake. Tyr–O• proves to be a major radical intermediate formed in proteins, in the order NCS > IgG > RBP; it is virtually missing in other proteins such as lysozyme (data not shown).

The 320–520-nm doublet and the 360-nm peak expected of the oxidized tryptophan radical (Posener et al., 1976) and of the histidine electron adduct (Steiner et al., 1985), respectively, are missing in the spectra. In fact, histidine reportedly reacts only very slowly with $CO_2^{\bullet -}$, and no mention of tryptophan oxidation by $CO_2^{\bullet -}$ has been made in the literature.

The determination of the bimolecular rate constant for phenoxyl plus disulfide radical anion formation was carried out with a large excess of protein (≥400 μM IgG or RBP, or ≥800 μM NCS) over the initial $CO_2^{\bullet -}$ concentration. The absorbance changes at 425–440 nm following the electron pulse then fitted an exponential time dependence. At lower protein concentration, the rate constants k_2 and k_3 in the competing reactions

$$2CO_2^{\bullet -} \rightarrow C_2O_4^{2-} \quad (1)$$

$$CO_2^{\bullet -} + \underline{S\text{–}S} \rightarrow CO_2 + \underline{S^{\bullet -}S} \quad (2)$$

$$CO_2^{\bullet -} + \text{Tyr–OH} \rightarrow HCOO^- + \text{Tyr–O}^\bullet \quad (3)$$

are low enough compared to k_1 [$(1.35 \pm 0.05) \times 10^9$ $M^{-1}\cdot s^{-1}$ experimental determination, consistently with literature data] for a substantial amount of $CO_2^{\bullet -}$ to decay via reaction 1 at doses per pulse larger than 5 Gy. The values of $k_2 + k_3$ and of the mean molar extinction coefficient ϵ_{pH8} determined under pseudo-first-order conditions are given in Table I.

Disulfide radical anions are prone to undergo reversible S–S bond rupture, yielding a thiyl radical intermediate:

$$\underline{S^{\bullet -}S} \underset{(-4)}{\overset{(4)}{\rightleftharpoons}} \underline{S^{\bullet}\ ^{-}S} \quad (4)$$

The equilibrium lies far to the left side in cyclic disulfides. With the exception of the inter-chain bonds in IgG, disulfide groups in the proteins considered here are cyclic systems in which the chains joining homologous cysteine groups are polypeptide segments. These loops are of varying length, polarity, and conformation and may exert closing or shearing forces. This may affect profoundly the open–closed form equilibrium 4, and hence the redox properties of the system and the absorptivity of the radical intermediate (von Sonntag, 1990).

(2.1.2) pH Dependence and Analysis of the Reaction in Acidic Medium. Figure 6 illustrates the pH dependence of the fate of radicals in RBP at 425 nm. Phase I, corresponding to radical formation at the expense of $CO_2^{\bullet -}$ was virtually unchanged between pH 8.2 and pH 7.5. Its apparent rate constant increased markedly upon further lowering the pH. The peak of absorbance at the buildup of phase I concomitantly exhibited a maximum between pH 7.5 and 6.5, except under true pseudo-first-order conditions, i.e., at high protein concentration ([RBP] ≥ 600 μM), and a rapid fall below pH 6 at any protein concentration. The time necessary for phase I to reach its maximum decreased with the pH, from ca. 200 μs at pH 8.25 down to 12 μs at pH 3.03 (Figure 6). The absorption spectrum taken at this maximum also changed with

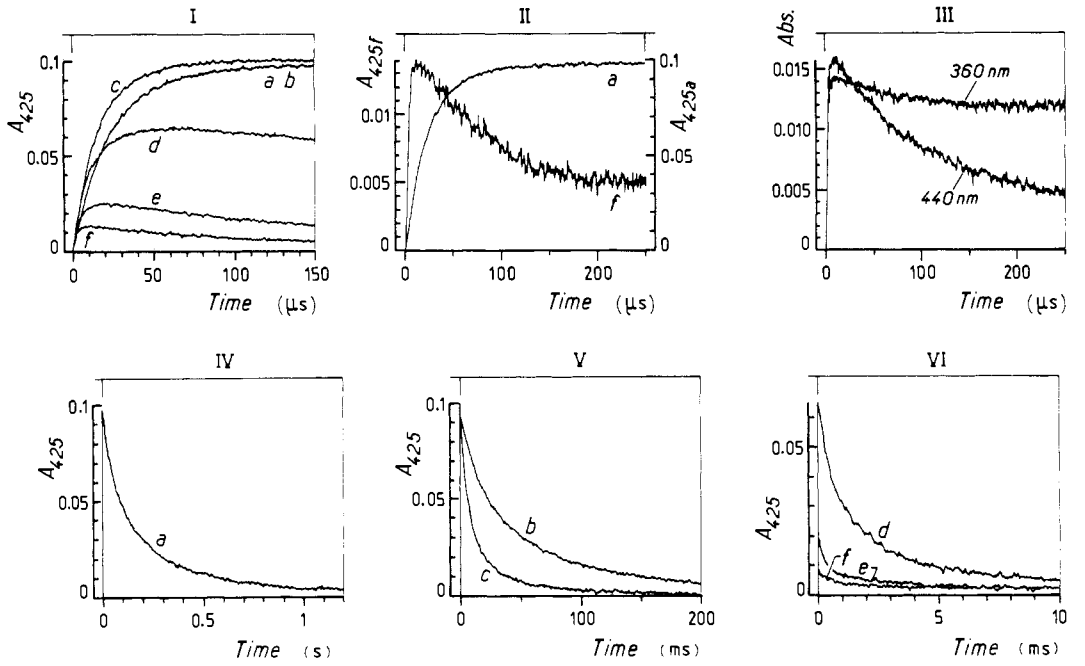

FIGURE 6: Digital oscilloscope recordings showing radical formation (I, II) and decay (IV–VI) in RBP (250 μM) at pH 8.25 (a), 7.10 (b), 6.11 (c), 5.12 (d), 4.06 (e), and 3.03 (f). The observation was fixed at 425 nm. Electron pulses were 36.9 ± 1.5 Gy. Nonidentical absorbance scales have been used for (a) and (f) in panel II in order to emphasize the difference in the time course of the reaction at pH extrema. For comparison, panel III shows phase I and phase II kinetics of IgG (500 μM IgG, pH 3.26, 52.2 ± 2.4 Gy pulses) at 360 and 440 nm.

pH, with a 25–35-nm blue shift upon acidification (Figure 5). The spectral properties of this intermediate, with a weak, broad band centered at 400 nm (Figure 5), are evocative of those reported for the protonated form of the disulfide radical anion, $(S\underline{\underline{\cdot}}S)H$ (Akhlak & von Sonntag, 1987). There was again no spectral evidence of radicals derived from tryptophan or histidine residues. The Tyr–O• absorption in the ultraviolet region was low comparatively to that found under neutral conditions, so that the contribution of the Tyr–O• absorption to the 400-nm band was minor. The increased rate (Table I) of sulfur-centered radical formation in acidic medium

$$CO_2^{\bullet -} + S\underline{\underline{\cdot}}S(+ H^+) \rightarrow CO_2 + (S\underline{\underline{\cdot}}S)H \qquad (5)$$

or in the sequence

$$CO_2^{\bullet -} + S\underline{\underline{\cdot}}S \rightarrow CO_2 + S\underline{\underline{\cdot}}\underline{\underline{\cdot}}S \qquad (2)$$

$$S\underline{\underline{\cdot}}\underline{\underline{\cdot}}S + H^+ \underset{(6)}{\overset{(-6)}{\rightleftharpoons}} (S\underline{\underline{\cdot}}S)H \qquad (6)$$

consistently occurs at the expense of tyrosine oxidization in reaction 3.

Radical formation and decay at pH 4.5 and below fitted quite nicely a biexponential model for 150–200 μs. This permitted us to carry out a precise deconvolution of phase I from subsequent radical breakdown, and hence a precise determination of the global rate constant k_{app} of protein free-radical formation through reactions 2, 3, 5, and 6 and of the bulk molar extinction coefficient ϵ_{app} relative to the primary species formed in the whole pH range investigated. Both ϵ_{app} and k_{app} experienced sigmoidal pH dependencies typical of acidic–basic equilibria (Figure 7). For NCS and RBP, ϵ_{app} and k_{app} fitted the same titration curve with pH as expected of the association–dissociation of a weak monovalent acid. The pH dependencies of ϵ_{app} and k_{app} for IgG were found by computer simulation to fit a system of (at least) three overlapping equilibria. The pK_a values deduced from ϵ_{app} values at the time of the pseudoequilibrium corresponding to the plateau of phase I (pK_E) differed from those obtained from k_{app} (pK_R) by 0.2–1.7 pH units (Table I).

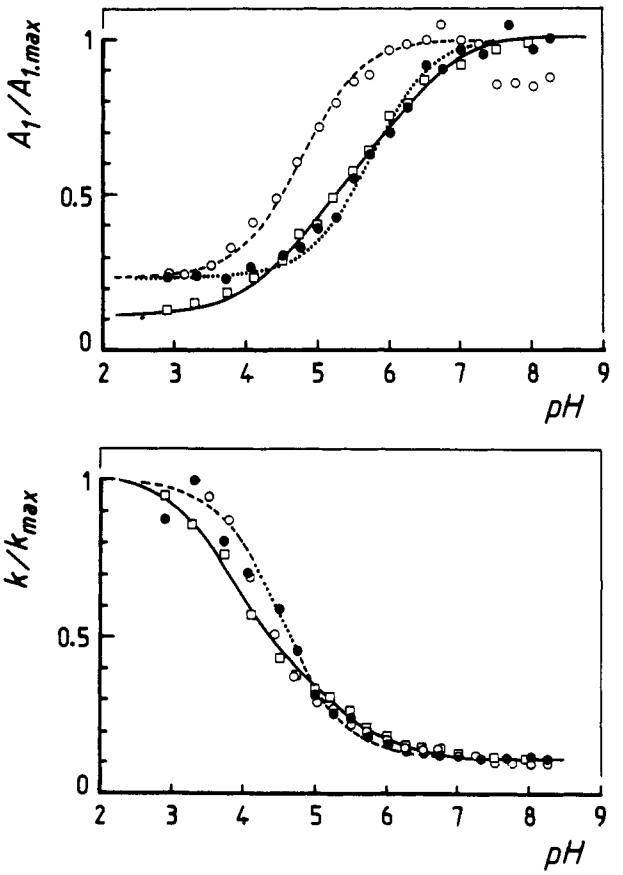

FIGURE 7: pH dependence of the relative rate constant (k/k_{max}) of phase I and of the relative amplitude of absorbance variation (A/A_{max}) at the buildup of phase I. NCS (●···) was 1 mM; IgG (□—) and RBP (○- - -) were 400 μM. The observation wavelength was fixed at 425 (NCS, RBP) or 440 nm (IgG). The dose per pulse was 42.2 ± 1.8 Gy. The curves have been calculated by using the pK_a values given in Table I.

Table II: Equilibrium and Rate Constants Relative to the Decay of the Radicals Formed in Proteins at Low pH (pH 3.28–3.36)[a]

	NCS	IgG	RBP
k_{II} (s^{-1})	9.1×10^3	10.3×10^3	10.2×10^3
k_7/k_{-7}	0.71 ± 0.02	0.85 ± 0.02	0.72 ± 0.03
k_9 ($M^{-1}\cdot s^{-1}$)	110 ± 30	110 ± 30	110 ± 30
ϵ(Cys–S$^\bullet$) ($M^{-1}\cdot cm^{-1}$)	170 ± 20	215 ± 25	290 ± 30

[a] Data treatment and calculations were performed as described in the text. k_{II} is the apparent rate constant corresponding to the reaction sequence 6–8. ϵ(Cys–S$^\bullet$) refers to the absorption of the thiyl radical intermediate (360 nm) at the plateau of phase II ($t \approx 0.4$–1 ms).

(2.2) Analysis of the Decay Phases of Radicals. (2.2.1) Reaction at pH 3.05–3.35. The bulk rate of radical decay increased substantially as the pH was lowered (Figure 7). At pH 4.5 and below, this decay process was biphasic (Figure 6). The primary radicals, presumably mostly in the form of (S$^\bullet$–S)H, first turned partly into a new species with a weak absorption peaking at 350–360 nm (Figure 5). This absorption is characteristic of a thiyl radical intermediate (Hoffman & Hayon, 1972, 1973; Akhlaq & von Sonntag, 1987). No residual Tyr–O$^\bullet$ persisted at this stage. The following scheme may therefore be proposed as an explanation of radical decay in acidic medium:

$$(S^{\bullet}\text{–}S)H \underset{(-6)}{\overset{(6)}{\rightleftharpoons}} S^{\bullet -}\text{–}S + H^+ \qquad (6)$$

$$(S^{\bullet}\text{–}S)H \underset{(-7)}{\overset{(7)}{\rightleftharpoons}} S^{\bullet}\ HS \qquad (7)$$

$$S^{\bullet -}\text{–}S + \text{Tyr–O}^{\bullet}(+ H^+) \rightarrow S\text{–}S + \text{Tyr–OH} \qquad (8)$$

In agreement with this scheme, the disulfide radical anion is a strongly reducing radical (Surdhar & Armstrong, 1986, 1987) while the phenoxyl radical Tyr–O$^\bullet$ is a good oxidant (DeFelippis et al., 1989). S$^\bullet$ HS is rather long-lived in proteins at completion of phase II. The forward rate constant to reaching this pseudoequilibrium state, k_{II} (Table II), was calculated by fitting the absorbance variations with time in phase I and phase II to a biexponential rate equation. k_{II} does not correspond to an elementary step. It is a function of the rate constants of reactions 6–8 and of the molar extinction coefficients of the intermediate radicals involved in these reactions. The equilibrium constant of reaction 7 was estimated from the ratio of the absorbance values taken at the buildup of phase I and at the plateau of phase II. k_6/k_{-6} can be deduced from the pK_E values given in Table I.

Both the open S$^\bullet$ HS and closed (S$^\bullet$–S)H form decayed slowly and concertedly in a reaction (phase III) whose apparent rate constant was proportional to the formate ion concentration. This is consistent with the oxidizing properties known from the thiyl radical (Morita et al., 1971; Elliot & Sopchyshyn, 1982; Elliot et al., 1984) which is always in equilibrium with the protonated disulfide radical anion (von Sonntag, 1990):

$$\{(S^{\bullet}\text{–}S)H \underset{(-7)}{\overset{(7)}{\rightleftharpoons}} S^{\bullet}\ HS\} + HCOO^- \rightarrow SH\ HS + CO_2^{\bullet -} \qquad (9)$$

The equilibrium and rate constants determined for these reactions are given in Table II.

(2.2.2) Kinetic Analysis of Phase II at pH 8.10–8.25. The kinetic analysis of radical decay at pH 8.10–8.25 was first performed by adjusting the radiation dose delivered in the electron pulse at between 2.2 and 37 Gy. The protein concentrations were taken high enough (300–500 μM) compared to the initial $CO_2^{\bullet -}$ concentration for the probability of attacking two sites in the same protein molecule to be less than 10^{-2}. The kinetic pattern was primarily dependent on the protein. With RBP, the apparent order of radical decay changed with the radiation dose, from a purely biexponential time dependence at doses of 2–5 Gy to a predominantly hyperbolic variation at high doses. The linear–quadratic system resulting from these competing reactions was solved by computer fitting of the absorbance data to the integral form of the rate equation, following a method similar to that described by Gorman and Connolly (1973). The dose dependence of the quadratic term was as expected of a second-order process. This process was highly dependent on the ionic strength. This second-order, bimolecular decay then should correspond to disproportionation of the disulfide radical anion, in agreement with Elliot et al. (1984) and Chan and Bielski (1973):

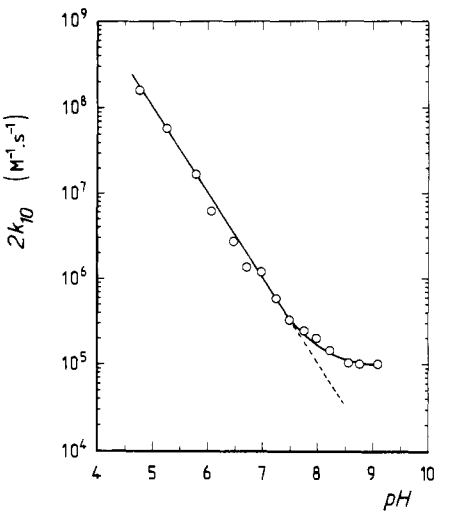

FIGURE 8: pH dependence of the disproportionation rate constant in RBP (425 nm, 20 mM phosphate–100 mM formate buffer, $I \approx 0.16$). RBP was 400 μM. The dose per pulse was 42.0 ± 3.7 Gy.

$$S^{\bullet -}\text{–}S + S^{\bullet -}\text{–}S(+ 2H^+) \rightarrow S\text{–}S + SH\ HS \qquad (10)$$

Phenoxyl radicals Tyr–O$^\bullet$ appear to be also able to undergo disproportionation (Feitelson & Hayon, 1973). The products of this reaction

$$\text{Tyr–O}^{\bullet} + \text{Tyr–O}^{\bullet}\ (+ H_2O) \rightarrow \text{products} \qquad (11)$$

have not been characterized. One could thus expect that the apparent rate constant of dismutation is a linear combination of $2k_{10}$ and $2k_{11}$. However, reaction 10 appears to predominate. As a matter of fact, the apparent rate constant of disproportionation in RBP shows a steep pH dependence below pH 8.0 down to pH 4.8 (Figure 8), consistent with the need for proton uptake in reaction 10. Considering the oxidizing character of the thiyl radical in equilibrium with (S$^\bullet$–S)H (von Sonntag, 1990), it might also be proposed that rapid disproportionation results from the combination of the protonated and anionic forms of the disulfide-centered radical

$$(S^{\bullet}\text{–}S)H + S^{\bullet -}\text{–}S(+ 2H^+) \rightarrow S\text{–}S + SH\ HS \qquad (12)$$

but the development below pH 5 of competing fast processes involving the same intermediate leaves this question open. The thiyl radical intermediate formed in reaction 7 decays mostly via reaction 9 on the time scale of seconds and shows no

Table III: Apparent Rate Constants for the Main Pathways of Radical Decay Proposed at pH 8.10–8.25 (20 mM Phosphate, 100 mM Formate Buffer, $I \approx 0.156$)[a]

	NCS	IgG	RBP	prereduced?
$2k_{III} \approx 2k_{10}$ ($M^{-1}\cdot s^{-1}$)			$(3.3 \pm 0.4) \times 10^5$	no
$k_{IV.Inter}$ ($M^{-1}\cdot s^{-1}$)	$(1.1 \pm 0.3) \times 10^4$		4.1×10^4	no
$k_{IV.Intra}$ (s^{-1})	5.2 ± 1.0	14.3 ± 1.5 (1) 94.3 ± 4.3 (2)	2.7	no
$k_{V.Inter}$ ($M^{-1}\cdot s^{-1}$)	$(2.5 \pm 0.2) \times 10^3$		6×10^5	yes
$k_{V.Intra}$ (s^{-1})	0.70 ± 0.08	44 (1) 185 (2)		yes

[a] These apparent rate constants correspond to the sum of reactions 10 and 11 (k_{III}), of reactions 13, 14, and 18 (k_{IV}), and of the whole processes, including reactions 14 and 23, which contribute to radical decay in prereduced samples (k_V). Rate constants were calculated by deconvolution of mixed-order processes in the bulk absorbance variations forming phase II and checked by initial rate analysis. The subscripts "Inter" and "Intra" refer to bimolecular (intermolecular) and monomolecular (intramolecular) processes, respectively. Second-order rate constants are given relative to the total protein concentration and are calculated by using the mean extinction coefficient at the maximum absorption wavelength. Data were obtained from pulse radiolysis experiments by monitoring the dose per pulse or the protein or the formate ion concentration, or by using partly reduced samples prepared by γ-ray preirradiation.

tendency to undergo rapid disproportionation. Though commonly observed with free tyrosine (Butler et al., 1984), 2,2′-biphenyl derivatives occurring by cross-linking between two phenoxyl radical moieties were apparently missing here. The only evidence of protein dimerization following $CO_2^{\bullet -}$ attack was obtained from RBP, and in that particular instance the dimeric material was totally cleaved upon exposure to 2-mercaptoethanol, indicative of intermolecular S–S bond formation. $\underline{S^{\bullet -}S}$ and Tyr–O$^\bullet$ should be equally weighted among distinct protein molecules for reaction 8 to appear as a hyperbolic pattern.

NCS and IgG showed no dismutation reaction at all. Phase II with NCS and IgG always fitted a biexponential rate equation in which the apparent rate constants were independent on the radiation dose per pulse. Among the two exponential functions constitutive of phase II for NCS, the apparent rate constant of one exponential term ($k_{IV.Inter}$) was proportional to the protein concentration. The other exponential term ($k_{IV.Intra}$) was invariant in this experiment. This prompts one to consider that radical decay in NCS results from an intramolecular (first-order) reorganization competing with a nondismutative bimolecular (pseudo-first-order) reaction between the disulfide anion or phenoxyl radical intermediates and groups in the native protein present in large excess. The effect of ionic strength on phase II for NCS was investigated in order to further substantiate this scheme. This was done by increasing stepwise the formate ion concentration up to 320 mM at constant pH and phosphate (20 mM) concentration. Only the rate constant relative to the bimolecular process was altered by changes in the ionic strength, as expected.

The time dependence of disulfide radical decay in RBP at low doses per pulse was analyzed in the same way and showed a situation similar to that found for NCS, with bimolecular and intramolecular terms competing with each other (Table III). Both exponential terms relative to phase II for IgG were absolutely independent of the protein concentration and of the formate ion concentration as well. Therefore, radical decay in IgG proceeds only from two parallel intramolecular reactions. The chemical mechanisms by which these nondismutative processes may occur are manifold. We shall consider here four main possibilities.

(1) The phenoxyl radical is an oxidant. This and the well-known ability of simple alkyl disulfides to undergo oxidation yielding a disulfide radical cation (Möckel et al., 1974; Bonifacic et al., 1975; Bonifacic & Asmus, 1975) suggest that Tyr–O$^\bullet$ might react by abstracting an electron from disulfide groups inter- or intramolecularly:

$$\text{Tyr–O}^\bullet + \underline{\text{S–S}}(+ \text{H}^+) \rightarrow \text{Tyr–OH} + \underline{\text{S}^{\bullet +}\text{S}} \qquad (13)$$

We would also tentatively propose that a similar process might occur by electron transfer between a disulfide group and the thiyl radical formed in equillibrium 4:

$$\underline{\text{S}^\bullet\ {}^-\text{S}} + \underline{\text{S–S}}(+ 2\text{H}^+) \rightarrow \underline{\text{SH HS}} + \underline{\text{S}^{\bullet +}\text{S}} \qquad (14)$$

Unfortunately the peak of absorption of the disulfide radical cation is at 420–450 nm (Bonifacic et al., 1975), i.e., close to those of $\underline{S^{\bullet -}S}$ and Tyr–O$^\bullet$, thus making its spectral characterization virtually impossible. With these caveats in mind, we still tentatively propose with Tung and Stone (1974, 1975) that $\underline{S^{\bullet +}S}$ should decay rapidly by hydrolysis, leaving a compound bearing sulfenic acid and thiyl radical termini, followed by reaction with formate and by dehydration regenerating the closed disulfide:

$$\underline{\text{S}^{\bullet +}\text{S}} + \text{H}_2\text{O} \rightarrow \underline{\text{S}^\bullet\ \text{HOS}} + \text{H}^+ \qquad (15)$$

$$\underline{\text{S}^\bullet\ \text{HOS}} + \text{HCOO}^- \rightarrow \underline{\text{SH HOS}} + \text{CO}_2^{\bullet -} \qquad (16)$$

$$\underline{\text{SH HOS}} \rightarrow \underline{\text{S–S}} + \text{H}_2\text{O} \qquad (17)$$

The chance that reaction 17, also proposed in other systems (Purdie, 1967; Quintiliani et al., 1977; von Sonntag, 1987), will occur at an increased rate in proteins should depend on the flexibility of the amino acid chain holding the terminal sulfur atoms in close proximity to each other. The $CO_2^{\bullet -}$ radical formed in reaction 16 may take a part in the chain reaction developing at pH 8.

(2) In addition to the initial formation of Tyr–O$^\bullet$ in reaction 3, Tyr–O$^\bullet$ might be generated in the course of phase II by reaction of tyrosine with the thiyl radical intermediate resulting from the equilibrium 4:

$$\underline{\text{S}^\bullet\ {}^-\text{S}} + \text{Tyr–OH} \underset{(-18)}{\overset{(18)}{\rightleftharpoons}} \underline{\text{SH}\ {}^-\text{S}} + \text{Tyr–O}^\bullet \qquad (18)$$

Electron transfer from Tyr–O$^\bullet$ to tryptophan residues

$$\text{Tyr–O}^\bullet + \text{TrpH} \underset{(-19)}{\overset{(19)}{\rightleftharpoons}} \text{Tyr–OH} + \text{Trp}^\bullet \qquad (19)$$

might also occur. However, given the redox potentials of the Trp$^\bullet$/TrpH ($E^{\circ\prime} \approx +1.05$ V), Tyr–O$^\bullet$/Tyr–OH ($E^\circ \approx +0.94$ V), and Cys–S$^\bullet$/Cys–SH ($E^\circ \approx +0.84$ V) couples (Surdhar & Armstrong, 1986, 1987; DeFelippis et al., 1989), equilibria 18 and 19 should lie far to the left side in proteins where redox centers are fixed in both their position in space and their relative stoichiometry. Pulse radiolysis investigations on model

peptides (Bobrowski et al., 1990) have shown that, except under strongly alkaline conditions (Butler et al., 1986; Harriman, 1987), reaction −19 prevails over the forward reaction 19. Furthermore, we found no spectral evidence of a metastable or transient Trp$^\bullet$ intermediate at 320–330 or 520–570 nm.

(3) γ-Ray experiments suggest that, except at low pH, cysteine free thiol groups may interfere with $CO_2^{\bullet -}$-induced processes. This reaction does not occur initially, i.e., starting from the native proteins. A pulse radiolysis analysis of this possibility thus requires prereduction of the proteins. Partial reduction of the disulfide bonds in RBP, IgG, or NCS by γ-ray irradiation preceding pulse radiolysis caused a significant increase in the rate and yield of formation of the disulfide radical anion at pH 8.10–8.25. This suggests that $CO_2^{\bullet -}$-induced oxidation of sulfhydryl groups

$$\underline{\text{SH HS}} + CO_2^{\bullet -} \rightarrow \underline{\text{S}^\bullet \text{ HS}} + HCOO^- \qquad (20)$$

and subsequent recyclization via reactions 7, 6, and 4 do occur and that reaction 20 is faster than reactions 2 and 3, consistent with the high rate constant of H$^\bullet$ abstraction from 1,4-dithiothreitol (8.3×10^8 $M^{-1}\cdot s^{-1}$) (Akhlaq et al., 1987) or glutathione ($\approx 10^9$ $M^{-1}\cdot s^{-1}$) (Z. Abedinzadeh and C. Houée-Levin, in preparation) to $CO_2^{\bullet -}$. Reduction of Tyr–O$^\bullet$ may also occur:

$$\underline{\text{SH HS}} + \text{Tyr–O}^\bullet \rightarrow \underline{\text{S}^\bullet \text{ HS}} + \text{Tyr–OH} \qquad (21)$$

and will end in the same product so that, in prereduced systems at neutral pH, the disulfide radical anion appears to be the only radical species present 200–400 μs following the electron pulse. This affects deeply the pattern of phase II. Phase II in prereduced NCS followed again a biexponential time dependence but, possibly for lack of the Tyr–O$^\bullet$ radical, there was a considerable decrease of the reaction rate. In contrast, phase II in the case of prereduced IgG and RBP was substantially more rapid than observed starting from the native proteins (Table III). In order to make sure that this effect did not proceed from bulk conformational changes, a half-reduced sample of RBP was prepared by γ-ray irradiation, alkylated with iodoacetamide, purified (see Experimental Procedures), and finally adjusted to a total protein concentration of 600 μM, i.e., to an uncleaved disulfide concentration equivalent to that of a 300 μM native RBP sample taken as reference. The phase I and phase II kinetics obtained from pulse radiolysis of this reduced–alkylated sample were identical within 10% with those of the reference, so that it seems firmly established that protein-bound free thiols are able to cross-react with the disulfide radical anion or its thiyl radical congener. The reaction

$$\underline{\text{S}^{\bullet -}\text{S}} + \underline{\text{SH HS}}(+ H^+) \rightarrow \underline{\text{S–S}} + \underline{\text{SH HS}} + H^\bullet \qquad (22)$$

acting catalytically would initiate a futile cycle and thus account for the gradual inhibition of Cys–SH formation observed under γ-ray irradiation with IgG and RBP as the integral radiation dose is raised (Figure 1). However, this hypothesis should be discarded because the activation energy required from reaction 22 is too high for it to proceed on the time scale of our experiments (C. von Sonntag, personal communication). At the present time we have no satisfactory explanation of how Cys–SH may interfere with the kinetics of disulfide radical anion decay.

(4) $CO_2^{\bullet -}$-induced cross-linking was observed with partly reduced RBP. It may result from thiyl radical recombination as proposed by others (Schuessler & Freundl, 1983; Elliot et al., 1984):

$$\underline{\text{S}^{\bullet -}\text{S}} + \underline{\text{S}^{\bullet -}\text{S}}(+ H^+) \rightarrow \overline{\text{SH S}}\text{—}\underline{\text{S–S}} \qquad (23)$$

Cross-linking might also occur via sulfuranyl radical intermediates by reaction between thiyl radicals and thiols in the same way as observed upon laser flash photolysis of 1,3-bis(alkylthio)propanes (Anklam & Steenken, 1988). In any case, cross-linking within the IgG complex will escape observation. Protein–protein cross-linking is not observed with NCS, presumably for lack of the interactions providing an adequate close contact between the reaction partners.

Conclusion

Disulfide bonds in proteins are readily reduced by the carboxyl radical. This is not, however, the sole reaction resulting from $CO_2^{\bullet -}$ attack. We saw that $CO_2^{\bullet -}$ is able to induce rapid one-electron oxidation of protein-bound cysteine free thiols and of tyrosine phenolic groups. The decay of these intermediate radicals via intramolecular and/or intermolecular processes is exceedingly complex and appears to differ widely among different proteins. Much remains to be done before a complete set of differential equations correlating the data obtained from pulse radiolysis and γ-ray irradiation experiments can be established and solved. However, notwithstanding the complexity of the reaction, the radiolytic method described here may find practical applications. It enables one to perform stepwise cleavage and subsequent alkylation of disulfide bonds in proteins with ease and reliability. Complete recovery of pure protein material in the native form makes the method of interest for the treatment of small aliquots. In such micro methods phosphate can be omitted, and formate and oxalate traces can be readily eliminated by reverse-phase chromatography. We shall report elsewhere on the use of this method for the preparation of functional monoclonal IgG fragments, for fluorescent or radioactive labeling by thiol-specific reagents, for conjugation of heterobifunctional agents, and for the preparation of chimeric protein heterodimers. This simply requires γ-ray irradiation in formate buffer under an N_2O atmosphere at pH between 4 and 8, slightly acidic conditions providing a more efficient chain reaction.

The thiyl radical $\underline{\text{S}^\bullet \text{ HS}}$ is a major intermediate in proteins at low pH. It decays in a reaction whose absolute rate depends directly on the formate ion concentration. Thiyl radical reduction to the sulfhydryl level by reaction with excess formation in reaction 9 regenerating 1 mol of the $CO_2^{\bullet -}$ radical is therefore proposed. This reaction accounts for chain initiation in acidic medium. Limited S–S bond cleavage may also occur in equilibrium with the disulfide radical anion in reaction [4] and account for the less efficient chain found at neutral pH (Figure 3). Interestingly, the equilibrium 4 represents a crossover between a strong reductant, the disulfide radical anion [E°(RSSR/RSSR$^{\bullet -}$) ≈ -1.3 V], and a strong oxidant, the thiyl radical [E°(RS$^\bullet$/RSH) $\approx +0.84$ V] (Surdhar & Armstrong, 1986, 1987). The open–closed form equilibria 4 and 7 do not necessarily imply large rearrangements of the protein structure, and such equilibria are known to occur in nonprotein cyclic disulfides (von Sonntag, 1987; Akhlaq & von Sonntag, 1987; Prütz et al., 1989; von Sonntag, 1990). However, the kinetic properties of these radical intermediates in proteins may differ widely from those found in low molecular weight compounds. In particular, k_{-7} in proteins (Table I) appears to be lower than found with dithiothreitol (Akhlaq & von Sonntag, 1987) by 2 orders of

magnitude. This is supposed to result from constraints introduced by the proteins in view of the properties known of the open–closed form equilibria involving thiyl radical intermediates (von Sonntag, 1990).

The titration curves drawn from the absorbance values taken at the buildup of primary radical formation in NCS and RBP (Figure 7) show the same profile as expected of a single acidic group. This ionic equilibration occurs in the same range of pK_a values (pK_E, Table I) as reported for low molecular weight disulfide compounds (Chan & Bielski, 1973; Redpath, 1973; Elliot & Sopchyshyn, 1982; Akhlaq & von Sonntag, 1987) and is presumed to correspond to protonation–deprotonation of the primary disulfide-centered radical in equilibrium 6. The pattern obtained from IgG is consistent with the existence of three groups with nonidentical ionization constants. This suggests that IgG offers three sites for reaction with $CO_2^{\bullet -}$ and that the resulting disulfide-centered radicals differ in their acidic–basic properties, due to environmental steric or hydrogen-bonding effects.

A similar pH dependence can be drawn from the apparent rate constants of radical formation in the proteins. The pK_a values (pK_R, Table I) thus calculated are close to those of glutamic or aspartic acid (NCS, RBP, IgG) and of histidine (IgG) residues. The meaning of these results is uncertain. It may indicate the formation of a complex held mainly by heteropolar interactions between the $CO_2^{\bullet -}$ anion and positively charged groups in the proteins, and labilized by the presence of negative charges. This would explain the considerable increase (Figure 6, Table I) in the rate of $CO_2^{\bullet -}$ uptake by proteins observed upon lowering the pH from 8.10–8.25 ($k_2 + k_3$) down to 2.9–3.3 (k_1). The objection may also be raised that, even though if it is diffusion-controlled (Akhlaq & von Sonntag, 1987), proton equilibration is not achieved at the initial times of primary protein radical formation, so that pK_R (and possibly pK_E) values are in fact complex parameters involving the rate constants of proton uptake. Experiments are in progress to elucidate this point.

The occurrence of disulfide radical anion disproportionation in proteins has been established by Sommer et al. (1982), who found it to proceed with rate constants in the range of 10^6–10^8 $M^{-1}\cdot s^{-1}$ under conditions of low salt concentration. Experiments performed by monitoring the formate ion concentration at pH 8.10–8.25 yielded a disproportionation rate constant as low as 3.5 $M^{-1}\cdot s^{-1}$ for RBP at null ionic strength. NCS and IgG showed no disproportionation reaction. This parallels the lack of cross-linking via reaction 23 in NCS and suggests that the interprotein contact areas involved in reaction 10 may be distinct from those in reactions 13, 14, 18, 21, and 23. Moreover, disproportionation is subject to a marked kinetic pH effect (Figure 8). General acidic–basic catalysis is relevant to this effect. It may be explained by protonation at the level of intermediate complexes modulating their electronic properties, hence modifying the activation energy barrier for asymmetric splitting yielding products, in the same way as in flavin dismutation (Favaudon & Lhoste, 1975).

Most of the reactions involved in the decay of $\underline{S^{\bullet -}S}$ and Tyr–$O^{\bullet}$ in proteins imply intramolecular or intermolecular long-range electron transfer. Such transfer is determined, among other factors, by the separation distance between redox partners and by their mutual orientation. This makes these reactions of interest for probing electron tunneling (Prütz et al., 1981; Faraggi & Klapper, 1988) within monomeric proteins or for studying the structure of binary or multimeric protein complexes devoid of electron-affinic cofactors. The ability to quantitate such behavior by pulse radiolysis would permit the investigation of reaction barrier shape and protein dynamics. Still more important, this might also be relevant to the outstanding question of free-radical repair of radiation-induced DNA lesions in deoxyribonucleoprotein structures (Prütz, 1989).

Acknowledgments

We thank Maurice Petit and Jean-Michel Lentz for the construction of the mechanical parts and electronic circuitry, Dr. Daniel Lavalette for his help in the design of the optical detection, and Christiane Dorey for skillful assistance in protein titration and electrophoresis experiments. We are greatly indebted to Prof. Clemens von Sonntag, Prof. Christiane Ferradini, and Prof. Monique Gardès-Albert for kind advice and helpful discussion.

Registry No. NCS, 101359-79-9; $CO_2^{\bullet -}$, 14485-07-5.

References

Adams, G. E. (1967) *Curr. Top. Radiat. Res. 3*, 35–93.
Adams, G. E., Redpath, J. L., Bisby, R. H., & Cundall, R. B. (1972) *Isr. J. Chem. 10*, 1079–1093.
Akhlaq, M. S., & von Sonntag, C. (1987) *Z. Naturforsch. 42c*, 134–140.
Akhlaq, M. S., Schuchmann, H. P., & von Sonntag, C. (1987) *Int. J. Radiat. Biol. 51*, 91–102.
Akhlaq, M. S., Murthy, C. P., Steenken, S., & von Sonntag, C. (1989) *J. Phys. Chem. 93*, 4331–4334.
Anklam, E., & Steenken, S. (1988) *J. Photochem. Photobiol. 43*, 233–235.
Bansal, K. M., & Fessenden, R. W. (1976) *Radiat. Res. 67*, 1–8.
Bent, D. V., & Hayon, E. (1975) *J. Am. Chem. Soc. 97*, 2599–2606.
Blankenhorn, G., Osuga, D. T., Lee, H. S., & Feeney, R. E. (1975) *Biochim. Biophys. Acta 386*, 470–478.
Bobrowski, K., Wierzchowski, K. L., Holcman, J., & Ciurak, M. (1990) *Int. J. Radiat. Biol. 57*, 919–932.
Bonifacic, M., & Asmus, K.-D. (1976) *J. Phys. Chem. 80*, 2426–2430.
Bonifacic, M., Schäfer, K., Möckel, H., & Asmus, K.-D. (1975) *J. Phys. Chem. 79*, 1496–1502.
Bradford, M. M. (1976) *Anal. Biochem. 72*, 248–254.
Butler, J., Land, E. J., Swallow, A. J., & Prütz, W. A. (1984) *Radiat. Phys. Chem. 23*, 265–270.
Butler, J., Land, E. J., Prütz, W. A., & Swallow, A. J. (1986) *J. Chem. Soc., Chem. Commun.*, 348–349.
Caspari, G., & Granzow, A. (1970) *J. Phys. Chem. 74*, 836–389.
Chan, P. C., & Bielski, B. H. J. (1973) *J. Am. Chem. Soc. 95*, 5504–5508.
DeFelippis, M. R., Murthy, C. P., Faraggi, M., & Klapper, M. H. (1989) *Biochemistry 28*, 4847–4853.
Elliot, A. J., & Sopchyshyn, F. C. (1982) *Radiat. Phys. Chem. 19*, 417–426.
Elliot, A. J., Simsons, A. S., & Sopchyshyn, F. C. (1984) *Radiat. Phys. Chem. 23*, 377–384.
Ellman, G. L. (1958) *Arch. Biochem. Biophys. 74*, 443–450.
Faraggi, M., & Klapper, M. H. (1988) *J. Am. Chem. Soc. 110*, 5753–5756.
Favaudon, V. (1983) *Biochimie (Paris) 65*, 593–607.
Favaudon, V., & Lhoste, J.-M. (1975) *Biochemistry 14*, 4731–4738.
Favaudon, V., Charnas, R. L., & Goldberg, I. H. (1985) *Biochemistry 24*, 250–259.

Feitelson, J., & Hayon, E. (1973) *J. Phys. Chem. 77*, 10–15.
Gibson, B. W., Herlihy, W. C., Samy, T. S. A., Hahm, K.-S., Maeda, H., Meienhofer, J., & Biemann, K. (1984) *J. Biol. Chem. 259*, 10801–10806.
Gorman, D. S., & Connolly, J. S. (1973) *Int. J. Chem. Kinet. 5*, 977–989.
Goto, Y., & Aki, K. (1984) *Biochemistry 23*, 6736–6744.
Hamazume, Y., Mega, T., & Ikenaka, T. (1984) *J. Biochem. (Tokyo) 95*, 1633–1644.
Harriman, A. (1987) *J. Phys. Chem. 91*, 6102–6104.
Hoffman, M. Z., & Hayon, E. (1972) *J. Am. Chem. Soc. 94*, 7950–7957.
Hoffman, M. Z., & Hayon, E. (1973) *J. Phys. Chem. 77*, 990–996.
Karmann, W., Granzow, A., Meissner, G., & Henglein, A. (1969) *Int. J. Radiat. Phys. Chem. 1*, 395–405.
Koppenol, W. H., & Rush, J. D. (1987) *J. Phys. Chem. 91*, 4429–4430.
Kozik, A. (1982) *Eur. J. Biochem. 121*, 395–400.
Kumosinski, T. F., Pessen, H., & Farrell, H. M. (1982) *Arch. Biochem. Biophys. 214*, 714–725.
Maeda, H., Glaser, C. B., Kuromizu, K., & Meienhofer, J. (1974) *Arch. Biochem. Biophys. 164*, 379–385.
Möckel, H., Bonifacic, M., & Asmus, K.-D. (1974) *J. Phys. Chem. 78*, 282–284.
Morita, M., Sasai, K., Tajima, M., & Fujimaki, M. (1971) *Bull. Chem. Soc. Jpn. 44*, 2257–2258.
Posener, M. L., Adams, G. E., Wardman, P., & Cundall, R. B. (1976) *J. Chem. Soc., Faraday Trans. 1 72*, 2231–2239.
Povirk, L. F., Dattagupta, N., Warf, B. C., & Goldberg, I. H. (1981) *Biochemistry 20*, 4007–4014.
Press, W. H., Flannery, B. P., Tezukolsky, S. A., & Vetterling, W. T. (1988) *Numerical Recipes*, pp 521–528, Cambridge University Press, Cambridge.
Prütz, W. A. (1989) *Int. J. Radiat. Biol. 56*, 21–33.
Prütz, W. A., Land, E. J., & Sloper, R. W. (1981) *J. Chem. Soc., Faraday Trans. 1 77*, 281–292.
Prütz, W. A., Butler, J., Land, E. J., & Swallow, A. J. (1989) *Int. J. Radiat. Biol. 55*, 539–556.
Purdie, J. W. (1967) *J. Am. Chem. Soc. 89*, 226–230.
Quintiliani, M., Badiello, R., Tamba, M., Esfandi, A., & Gorin, G. (1977) *Int. J. Radiat. Biol. 32*, 195–202.
Rao, D. N. R., Symons, M. C. R., & Stephenson, J. M. (1983) *J. Chem. Soc., Perkin Trans. 2*, 727–730.
Redpath, J. L. (1973) *Radiat. Res. 54*, 364–374.
Schuessler, H., & Freundl, K. (1983) *Int. J. Radiat. Biol. 44*, 17–29.
Sommer, J., Jonah, C., Fukuda, R., & Bersohn, R. (1982) *J. Mol. Biol. 159*, 721–744.
Steiner, J. P., Faraggi, M., Klapper, M. H., & Dorfman, L. M. (1985) *Biochemistry 24*, 2139–2146.
Surdhar, P. S., & Armstrong, D. A. (1986) *J. Phys. Chem. 90*, 5915–5917.
Surdhar, P. S., & Armstrong, D. A. (1987) *J. Phys. Chem. 91*, 6532–6537.
Surdhar, P. S., Mezyk, S. P., & Armstrong, D. A. (1989) *J. Phys. Chem. 93*, 3360–3363.
Tung, T. L., & Stone, J. A. (1974) *J. Phys. Chem. 78*, 1130–1133.
Tung, T. L., & Stone, J. A. (1975) *Can. J. Chem. 53*, 3153–3157.
Von Sonntag, C. (1987) *The Chemical Basis of Radiation Biology*, pp 353–374, Taylor & Francis, London, England.
Von Sonntag, C. (1990) in *Sulfur-Centered Reactive Intermediates in Chemistry and Biology* (Chatgilialoglu, C., & Asmus, K. D., Eds.) Plenum, New York (in press).
Willson, R. L. (1970) *J. Chem. Soc., Chem. Commun.*, 1425–1426.
Wu, Z., Ahmad, R., & Armstrong, D. A. (1984) *Radiat. Phys. Chem. 23*, 251–257.

Information Content of Amino Acid Residues in Putative Helix VIII of the *lac* Permease from *Escherichia coli*

Peter C. Hinkle,*,‡ Paul V. Hinkle,‡ and H. Ronald Kaback§
Roche Institute of Molecular Biology, Roche Research Center, Nutley, New Jersey 07110
Received July 17, 1990

ABSTRACT: Mutants in putative helix VIII of lactose permease that retain the ability to accumulate lactose were created by cassette mutagenesis. A mutagenic insert encoding amino acid residues 259–278 was synthesized chemically by using reagents contaminated with 1% each of the other three bases and ligated into a *KpnI/BclI* site in the *lacY* gene in plasmid pGEM-4. Mutants that retain transport activity were selected by transforming a strain of *Escherichia coli* containing a wild-type *lacZ* gene, but deleted in *lacY*, with the mutant library and identifying colonies that transport lactose on indicator plates. Sequencing of the mutated region in *lacY* in 129 positive colonies reveals 43 single amino acid mutations at 26 sites and 26 multiple mutations. The variable amino acid positions are largely on one side of the putative α-helix, a stripe opposite Glu269. This mutable stripe of low information content is probably in contact with the membrane phospholipids.

The lactose (*lac*) permease of *Escherichia coli* is a polytopic cytoplasmic membrane protein that catalyzes the simultaneous translocation of a single β-galactoside with a single H^+ (i.e., β-galactoside/H^+ symport or cotransport) (Kaback, 1989, 1990). The permease has been solubilized from the membrane, purified to homogeneity, and reconstituted into phospholipid vesicles (Newman et al., 1981; Viitanen et al., 1985) and is probably completely functional as a monomer (Costello et al., 1987). The *lacY* gene, which encodes the permease, has been

‡ Present address: Section of Biochemistry, Molecular and Cell Biology, Cornell University, Ithaca, NY 14853.
§ Present Address: Howard Hughes Medical Institute, Department of Physiology, Molecular Biology Institute, University of California School of Medicine, Los Angeles, CA 90024-1574.

0006-2960/90/0429-10989$02.50/0